Journal of Catalysis **200,** 345–351 (2001)
doi:10.1006/jcat.2001.3220, available online at http://www.idealibrary.com on IDEAL®

Thermal Removal of Ammonia from Mordenite

Ivan Jirka,[1] Jan Plšek, and Josef Kotrla

J. Heyrovský Institute of Physical Chemistry, Academy of Sciences of the Czech Republic, Dolejškova 3, 182 23 Prague 8, Czech Republic

Received November 20, 2000; revised February 9, 2001; accepted February 23, 2001; published online May 15, 2001

Two types of NH_4^+ cations can be distinguished in the surface layer of NH_4^+ mordenite by XPS, viz., NH_4^+ cations coordinated in the side pockets (22%) and in the main channels (78%). Additionally, nonframework SiO_x species were observed in the mordenite. Thermal activation of NH_4^+ mordenite at 400°C causes the appearance of two types of atomic nitrogen strongly chemisorbed on these SiO_x nonframework species. © 2001 Academic Press

Key Words: **X-ray photoelectron spectroscopy; zeolite; thermal activation.**

1. INTRODUCTION

The H forms of zeolites are solid acids widely used as catalysts (1). The H form of mordenite, investigated in this study, was proved to be catalytically active in various shape-selective reactions (1). H-zeolites are often prepared by thermal decomposition of their NH_4^+ forms (1, 2). Likewise, the acidic properties of H-zeolites are frequently estimated using NH_3 as a probe molecule. Moreover, the treatment of zeolites in a stream of ammonia was recently proposed as a promising technique for the preparation of a novel catalyst (3). Therefore, a detailed understanding of the interaction of the zeolite skeleton with ammonia is beneficial for characterization of its catalytic properties.

Information about the interaction of NH_3 with the skeleton of a zeolite has often been obtained by investigating the adsorption of NH_3 with the carefully dehydrated H form of the zeolite *in vacua* (4–8). Individual NH_4^+ (NH_3) sites in a zeolite show different vibrational activities due to their different local group symmetries. Thus, infrared spectroscopy (IR) is the most straightforward method for investigation of the coordination mode of NH_4^+ (NH_3) in zeolites. Adsorbed ammonia may be coordinated in the vicinity of Brønsted sites in the protonated form (NH_4^+ species) or coordinatively bonded to Lewis sites of the zeolite (NH_3 species). Several sites for the NH_4^+ ions (bidentate, tridentate) have been suggested in zeolites using quantum chemical calculations (see (9) and references therein). Diverse coordinations of NH_4^+ have been observed by IR in a variety of zeolites (4). However, the application of IR has several limitations. It requires carefully dehydrated zeolite samples. Intensive bands corresponding to vibrations of coadsorbed water overlap with NH_4^+ (NH_3) bands, particularly in the spectral region from 2400 to 3800 cm^{-1}. Moreover, the direct quantification of the distribution of nitrogen-containing species in different sites by IR is rather complicated.

X-Ray photoelectron spectroscopy (XPS) is another promising source of information on the siting of cations in zeolites (10, 18). Characterization of the sample by XPS is based on the interpretation of the core level binding energies E_b, lineshapes, and intensities of the photoelectron spectra. The coordination mode of NH_4^+ (NH_3) in the zeolite affects the extent of the positive charge on the N atom. The binding energy E_b of the N 1*s* photoelectron line measured by XPS is thus sensitive to the changes in the coordination mode of the nitrogen-containing species. Direct quantification of the degree of thermal deammoniation in the catalytically interesting subsurface region of the zeolite is available from the intensities of the N 1*s* photoelectron line. Moreover, in the case of a homogeneous sample this information is also representative of its bulk.

Thermal activation of NH_4^+ mordenite is investigated by XPS in this article. The disappearance of N–H bonds in the thermally treated sample is checked by IR. Together with IR and XPS, mass spectrometry (MS) has been used for the analysis of desorbed gases during the heat treatment of NH_4^+ mordenite.

2. EXPERIMENTAL

NH_4^+ mordenite was prepared from its Na form by repeated NH_4^+ ion exchange. The parent mordenite was synthesized at the Institute of Oil and Hydrocarbon Gases, Bratislava, Slovak Republic. The high crystallinity of the sample was checked by X-ray diffraction, infrared spectroscopy of skeletal vibrations, and measurement of the sorption capacity for Ar (11).

[1] To whom correspondence should be addressed.

0021-9517/01 $35.00

2.1. XPS Experiments

A small amount of the zeolite (typically less than 5 mg) was pressed into a tungsten gauze and mounted on the sample holder. The area of supported pellet prepared in this way was slightly larger than 1 cm^2 (this area slightly exceeded the irradiated area in the XPS experiment), and its thickness was ~0.1 mm. Such a form of sample minimizes charging problems that appear during XPS measurement. It also diminishes the temperature gradients existing when the sample is heated, as well as reduces the possible effects of readsorption of NH_3. The ESCA III Mk 2 (VG) spectrometer with hemispherical analyzer and twin (Al/Mg) anode was used in a fixed retardation ratio mode. The passing energy used was 50 eV, and the slit width of the analyzer was 4 mm. Photoelectrons were excited by nonmonochromatized Al$K\alpha_{1,2}$ characteristic X rays (240 W). The base pressure during the experiment was typically lower than 3×10^{-9} Torr. The spectra of NH_4^+ mordenite were measured after ~120 min of evacuation at ambient temperature, and after heat treatment at 400°C for 30, 60, and 210 min *in situ*. The Al 2*p* and Si 2*p* photoelectron spectra were curve fitted by one Gauss line, while two Gauss lines were used to fit the N 1*s* spectra. A linear background was subtracted. Experimental spectra were smoothed (FFT, 5 points) prior to the curve-fitting procedure. Binding energies E_b of the Al 2*p* and N 1*s* photoelectron lines were calibrated using the E_b of the Si 2*p* photoelectron line (E_b(Si 2*p*) = 103.4 eV) as proposed in the literature (12, 13). The concentration of N was estimated as a N/Al atomic ratio, evaluated from the integral intensities of the N 1*s* and Al 2*p* photoelectron lines, corrected by the pertinent values of the photoinization cross sections (14).

2.2. MS Experiments

Mass spectrometric analysis was carried out in a stainless-steel apparatus pumped by a turbomolecular pump at a base pressure of $\sim 10^{-6}$ Torr. The apparatus was equipped with a quadrupole mass unit QMU (Finnigan 400) which was differentially pumped by an ion getter pump (base pressure $\sim 10^{-8}$ Torr). The sample, pressed into a tungsten gauze, was spotwelded to a Ni foil. After overnight evacuation at ambient temperature it was resistively heated to 400°C, and left at this temperature for 210 min. The chemical composition of the residual atmosphere was measured during the heat treatment. The sample was then heated in a stepwise manner up to 450–800°C with increments of 50°C. The sample was kept 10 min at each temperature. Chemical analysis of the residual atmosphere was performed at each temperature 0, 5, and 10 min after its change. Masses (m/e) at 16, 17 and 18 a.u. were recorded. Masses 18 and 17 were used for detection of H_2O and NH_3, respectively (the latter was corrected for the concentration of H_2O). Application of the mass 16 gives identical results as that of $m/e = 17$. Measurement of temperature during the heat treatment was carried out with a W/Ta thermocouple attached at the center of the tungsten gauze. The temperature difference measured at the center of the gauze and at its edges did not exceed 20°C (for temperatures $T < 600$°C) and 60°C (at $T = 900$°C).

2.3. IR Experiments

Infrared spectra were measured on Nicolet MX 1E and Protégé 460 spectrometers. The sample in the form of self-supported pellet could be heated *in situ* in a vacuum ($\sim 10^{-4}$ Torr). Spectra were measured before and after ~30 min evacuation at ambient temperature and after ~30, ~90, and ~210 min at 400°C (±5°C).

3. RESULTS

3.1. IR Spectra

The two bands observed in the infrared spectrum of the NH_4^+ mordenite before evacuation at 1450 and 1625 cm^{-1} (see Fig. 1) have been assigned to NH_4^+ coordinated on Brønsted centers and NH_3 species on Lewis sites,

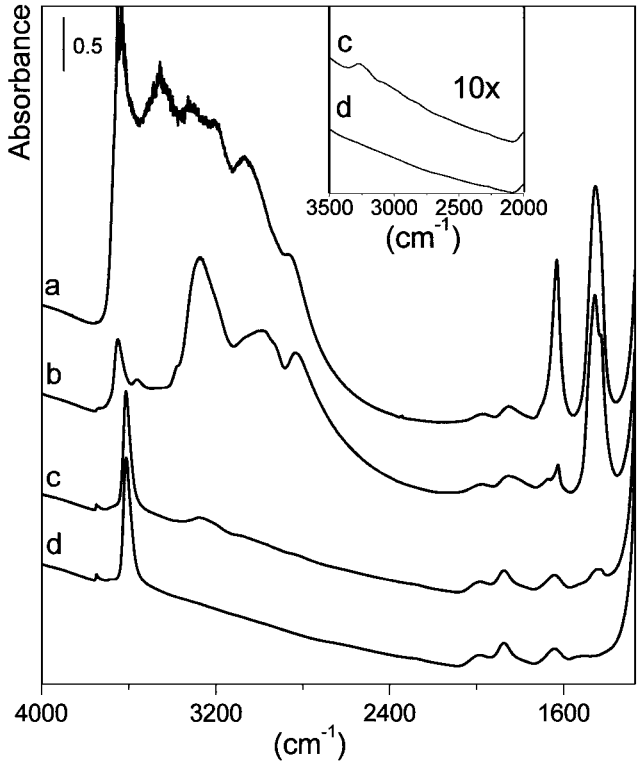

FIG. 1. Infrared spectra of the NH_4^+ mordenite in air (a), evacuated for 30 min at room temperature (b) and at 400°C for 30 min (c) and 210 min (d). The spectrum of the sample evacuated at 400°C overnight is identical to spectrum d (not shown in the figure). The region of N–H stretching vibrations (2000–3500 cm^{-1}) of spectra c and d is magnified in the inset to the figure.

TABLE 1

Binding Energies E_b (eV), Full Widths at Half-Maxima W (eV), and Intensities of Low- and High-Energy N 1*s* Photoelectron Lines N(1) and N(2) as Obtained by Curve Fitting of the N 1*s* Photoelectron Spectra[a]

t (min)	$E_b(1)$	$W(1)$	N(1)	$E_b(2)$	$W(2)$	N(2)	N(1) + N(2)
0	400.0	2.5	0.22	403.2	2.5	0.77	0.99
30	398.9	2.6	0.22	402.0	2.6	0.53	0.75
90	399.0	2.6	0.22	402.0	2.6	0.42	0.64
210	398.8	2.6	0.21	401.8	2.6	0.38	0.59

[a] E_b (eV) are calibrated using E_b of the Si 2*p* photoelectron line (103.4 eV (12, 13)); the intensities are normalized relative to the intensity of the Al 2*p* photoelectron line and pertinent values of photoionization cross sections.

respectively (5). However, the latter band overlaps with bands of physisorbed water (15). An intensity decrease in the infrared band at 1449 cm^{-1} and particularly at 1624 cm^{-1} is already evident after 30 min of evacuation at room temperature (Fig. 1). The decrease in the latter band is much more pronounced than the decrease in the former one. Heating the sample at 400°C in a vacuum for 30, 90, and 210 min causes the gradual disappearance of all the bands corresponding to N–H vibrations. Residual bands in the stretching region at 2500–3400 cm^{-1}, which remain in the spectrum of the mordenite evacuated at 400°C for 30 min (Fig. 1c), represent only a negligible amount of the remaining NH_x species coordinated on bridging sites of mordenite (<∼1%). The bands at 3605 and 3741 cm^{-1} appear as a result of ammonia removal and dehydration of the sample. These bands are assigned to the acidic and nonacidic hydroxyl groups of mordenite, respectively (7).

3.2. Photoelectron and MS Results

The N/Al atomic ratio of the parent sample, estimated from the pertinent photoelectron spectra, is equal to unity within experimental error (Table 1). A moderate decrease in the intensity of the N 1*s* line is induced by prolonged heating (210 min; see Table 1 and Fig. 2). The latter result is in agreement with the findings of the MS analysis of the thermally desorbed gases (Fig. 3). No changes in the chemical composition of the residual atmosphere

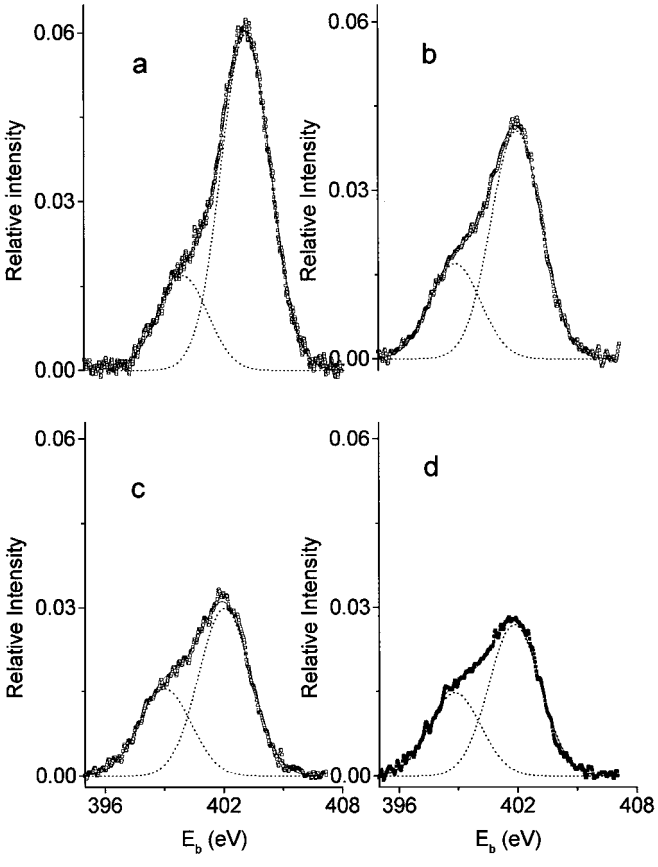

FIG. 2. The N 1*s* photoelectron spectrum of the NH_4^+ mordenite before heat treatment (a) and after heating at 400°C for 30 min (b), 90 min (c), and 210 min (d).

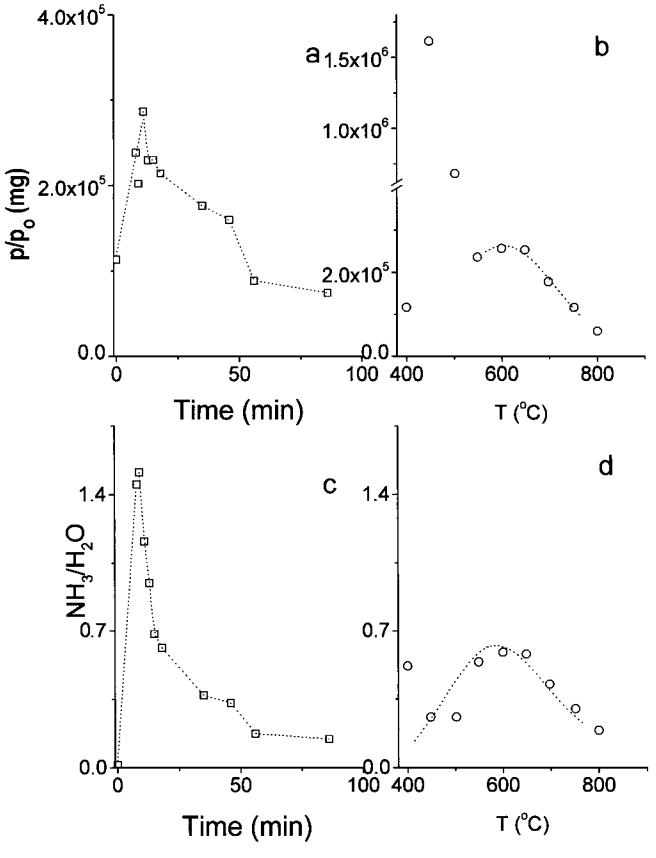

FIG. 3. Isothermal desorption of NH_3 at 400°C as a function of time measured by MS (a) followed by stepwise heating of the NH_4^+ mordenite to 800°C (b). The NH_3/H_2O ratio in the residual atmosphere during isothermal heating of the NH_4^+ mordenite at 400°C (c) followed by its stepwise heating to 800°C (d).

TABLE 2

Binding Energies E_b (eV) of the Al 2*p* Photoelectron Line and Full Widths at Half-Maxima *W* (eV) of the Al 2*p* and the Si 2*p* Photoelectron Lines as Obtained from the Curve Fitting[a]

t (min)	E_b (Al 2*p*)	*W* (Al 2*p*)	Si/Al	*W* (Si 2*p*)
0	74.9	2.50	9.0	2.60
30	74.9	2.525	8.9	2.6
90	74.9	2.20	9.6	2.2
210	75.0	2.20	9.5	2.2

[a] E_b of the Al 2*p* photoelectron line was calibarated by E_b of the Si 2*p* photoelectron line (103. 4 eV (12)).

after ~100 min of isothermal experiment were observed. Part of the nitrogen-containing species, however, was not desorbed from the sample at 400°C, even after 210 min of isothermal heating (Figs. 3a and 3c). A substantial amount of nitrogen-containing species (and water) desorbs by further nonisothermal heating above 400°C, following the preatreatment at 400°C (Figs. 3b and 3d). This result is in qualitative agreement with the findings of others (5).

No lineshape changes were observed in the Al 2*p* and Si 2*p* photoelectron spectra after sample heating; only some narrowing was detected (Fig. 4, Table 2). The binding energy E_b of the Al 2*p* photoelectron line equals 74.9 eV regardless of heat treatment (Table 2). A small increase in the Si/Al atomic ratio occurred on heating.

The N 1*s* photoelectron spectrum of the parent sample was curve fitted by two Gauss lines. The fitting procedure by 70% of a Gaussian and 30% of a Lorentzian line as proposed in the literature (13) gave similar results. Results of the curve fitting are summarized in Table 1. On heating, the binding energies E_b estimated for both lines are shifted by ~1 eV to lower values. No change in the width of the N 1*s* photoelectron lines was observed on heating. The influence of X-ray dose on the lineshape of the N 1*s* photoelectron spectra is negligible.

4. DISCUSSION

The correlation of XPS, MS and IR results should be carried out with caution because of the different depths of information provided by these methods. While IR and in this case also MS provide bulk information, XPS is surface sensitive (information depth ~5 nm (10)). However, some qualitative conclusions can be obtained from this correlation.

The temperature of the heat treatment was selected to minimize the creation of defect sites in the mordenite, as well as the concentration of $NH_4^+(NH_3)$ species. However, the occurence of some defect sites, both before and after heat treatment, particularly in the surface region of the mordenite, cannot in principle be excluded. Their possible presence is therefore discussed in the next paragraph. The effect of the coordination mode of the nitrogen-containing species on the N 1*s* photoelectron spectra before and after heat treatment is discussed thereafter.

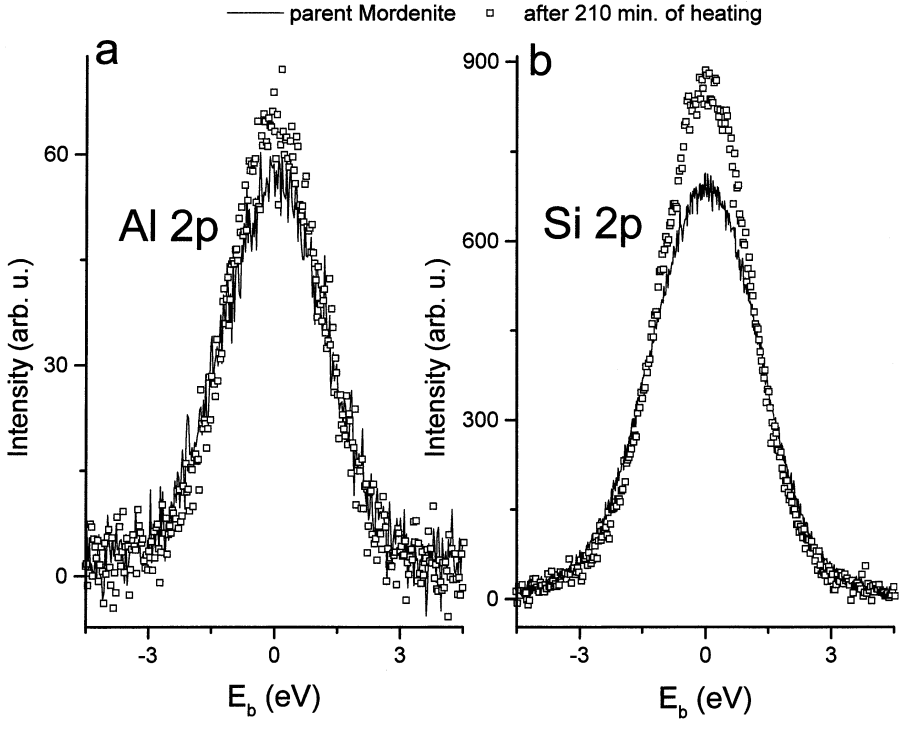

FIG. 4. Al 2*p* (a) and Si 2*p* (b) photoelectron spectra of the NH_4^+ mordenite before and after heat treatment.

4.1. Defect Sites

According to IR as well as XPS no defect sites associated with Al in mordenite were observed. The band at ~3660 cm^{-1} in the infrared spectrum has been assigned to nonskeletal OH species containing Al (16, 17). Its absence in the infrared spectrum of the mordenite even after overnight evacuation indicates the absence of substantial bulk skeletal dealumination of the mordenite when heat treated. Moreover, no significant bands of the Lewis acid sites were detected on adsorption of CD_3CN on overnight-heated (400°C) mordenite (11). These results are in agreement with the conclusions of Wichterlová *et al*. (28), who discussed an analogous problem quantitatively for ferrierites and MFI zeolites.

Only a moderate increase in the Si/Al ratio estimated by XPS relative to its bulk value (if any) occurred in the surface layer of mordenite. The bulk Si/Al atomic ratio is 8.5, while the surface value is equal to 9.0 (Table 2), i.e., the surface region of the parent mordenite seems to be slightly depleted of Al. The heat treatment causes a moderate increase in the Si/Al ratio, which is equal to ~9.6 after heating of the mordenite for 90 and 210 min (Table 2). The observed effects are close to the experimental error of the quantitative analysis by XPS, which has been proposed to be ~10 to ~15% (relative) (10). This error is generally caused by several factors, such as inadequate correction of the photoelectron line intensity ratio using the pertinent values of the inelastic mean free path $\lambda(E)$ and transmission function of the analyzer $T(E)$, and the problems associated with the proper subtraction of the inelastic background. These problems, however, are minimal in the case of the evaluation of the Si/Al ratio. The difference in the energies of the Si 2*p* and Al 2*p* photoelectron lines (~30 eV) is negligible and no correction on $\lambda(E)$ and (TE) is required. The problems associated with inelastic background subtraction are also minimal in this case (the spectra are narrow, and there is a negligible increase in the inelastic background intensity in the high-energy region of the spectrum). The error of estimation of the Si/Al ratio is thus probably lower than ~10%. Indeed, small changes in the chemical composition of the mordenite surface region are easily observable when the absolute values of the Si 2*p* and Al 2*p* photoelectron line intensities before and after heat treatment are compared (Fig. 4). While the intensity of the latter spectrum is not affected by heating, the intensity of the former increases. The enrichment of the mordenite surface on treatment with Si is evident. This effect is explicable as a consequence of the heat-induced migration of Si-containing species to the outer surface of the zeolite.

Tetrahedrally and octahedrally coordinated Al cannot be distinguished by photoelectron spectra. However, the presence of tricoordinated Al in the framework of the mordenite would affect the shape of the Al 2*p* photoelectron spectrum. The standard values of E_b (Al 2*p*) of Al(IV), (Al(VI)), and Al(III) are 74.7 and 75.4 eV (12), respectively. The latter line was not found at the resolution used in the spectrum. No lineshape changes followed heat treatment. The moderate narrowing of the Al 2*p* spectrum after 90 and 210 min of heat treatment can be explained by the change in the differential charging of the sample on heating. A similar narrowing was observed for the Si 2*p* photoelectron spectra (Table 2). Thus the defect sites (if any) are not predominantly associated with Al atoms. However, it seems reasonable to assume the presence of defect sites in nonframework Si-containing species, particularly after the heat treatment.

4.2. N 1s Photoelectron Spectra

Remy *et al*. (13) observed only one single line at 403.0 eV with a full width at half-maximum of 2.6 eV in the N 1*s* photoelectron spectrum of NH_4^+ mordenite with a Si/Al ratio similar to the ratio in the sample in our study. They assigned this line to NH_4^+ coordinated on Brønsted sites. A line at comparable E_b (403.2 eV, Table 2) was observed in the present work as well, but it is accompanied by a low-energy line at 400.0 eV. Both lines are assigned to NH_4^+ coordinated on Brønsted sites. The NH_4^+ molecule can be localized in the main channel of mordenite and in the side pockets. While the tetradental coordination of NH_4^+ was demonstrated in the small cavities of the mordenite (4), tridental and bidental coordination of NH_4^+ takes place in the main channel. More intimate connection of tetradentally coordinated NH_4^+ molecules with the skeleton of mordenite causes a decrease in the pertinent value of the N 1*s* binding energy in comparison with its value in less strongly bound bidentate and tridentate species. In this context we tried to fit the N 1*s* photoelectron spectrum by using more than two lines. This fitting procedure, however, does not give unambiguous results. Thus, the high-energy N 1*s* line is assigned to NH_4^+ coordinated in the main channel and the low-energy line to NH_4^+ in the side pockets. An alternative interpretation of the low- and high-energy lines in the N 1*s* photoelectron spectrum as being due to the coordination of a part of the nitrogen-containing species to Lewis sites in the parent mordenite is improbable. The E_b value of the N 1*s* photoelectron line assigned to nonprotonated ammonia coordinated on Lewis sites in the mordenite is equal to 399.1 eV (13), which is a substantially lower than the value of the low-energy N 1*s* line (400.0 eV). The infrared band observed at 1624 cm^{-1} (Fig. 1a) can thus be assigned solely to residual physisorbed water present in the NH_4^+ mordenite evacuated at room temperature. Most of the NH_4^+ cations are localized in the main channel of mordenite (78%), the rest in the side pockets.

The discrepancy between the N 1*s* lineshape observed for the nonheated sample in this work and that in (13) is explicable in terms of the inaccessibility of the sites in

small cavities for NH_4^+ ion exchange of the parent mordenite due to their blocking by extraframework Al species in the latter study. Indeed, a moderate increase in the surface concentration of Al in comparison with the bulk concentration ($(Si/Al)_{bulk} = 6.8$, $(Si/Al)_{surf.} = 5.8$) was observed in this work.

Evacuation of the NH_4^+ mordenite at 400°C caused a decrease in the intensity of the high-energy N 1*s* line while the intensity of the low-energy line remained constant. However, as is clear from the infrared bands, almost no N–H bonds are present in heated mordenite (Fig. 1d). A rather moderate decrease in the intensity of the N 1*s* photoelectron spectrum accompanied by disappearance of the infrared bands of the N–H vibrations was also observed for other zeolites (NH_4^+faujasite, NH_4^+ZSM-5, NH_4^+ferrierite (18, 19)). Thus, bare nitrogen atoms remain in the mordenite after heat treatment. Alternatively, in principle some residual NH_n species observed by XPS may remain only in the surface region of the mordenite. Their overall concentration would be negligible and so they could be detected solely by XPS. However, as follows from MS analysis of the thermally desorbed gases from mordenite, this explanation can be ruled out. The sample evidently contains a substantial amount of nitrogen-containing species even after isothermal heat treatment at 400°C for 210 min. The amount of NH_3 desorbed at temperatures higher than 400°C from mordenite pretreated in this way is well above the ~1% of the original NH_3 concentration that would follow from the IR data (Figs. 1, 3b, 3d). The apparent discrepancy between the IR and MS results may be explained as follows. The N atoms desorbed from mordenite react with OH groups created by dehydroxylation:

$$2N_{ads} + 6OH^{\bullet} \rightarrow 2NH_3 + 3O_2. \qquad [1]$$

It is reasonable to assume that atomic nitrogen is bonded on defect sites in the mordenite. It has been proved that the presence of oxygen vacancies in TiO_2 causes dissociative desorption of NH_3 (20). Atomic nitrogen is left behind in these vacancies. We thus propose that nitrogen atoms are bonded to Si-containing nonframework species, present in the voids of the mordenite.

Interaction of NH_3 with SiO_2 has already been thoroughly investigated (see, for example, Refs. 21–25). The occurrence of chemisorbed NH_3 indeed requires the presence of defect sites (21). However, the observed mechanism of thermal desorption of NH_3 from SiO_2 is rather different. In contrast to our results, the Si–NH_2 and Si–NH groups have elsewhere been identified as mesoproducts of thermal desorption by IR at temperatures above 400°C. These species were stable up to 900°C (21, 22). Introduction of atomic N into SiO_2 is typically carried out at temperatures as high as ~1000°C (23–25). Nitrogen is present in the form of nitride. The presence of atomic nitrogen in the form of dispersed nitride in heated mordenite can thus be excluded. Indeed, the E_b of the N 1*s* photoelectron line of bulk silicon nitride (Si_3N_4) is 398.1 eV (10), and for dispersed nitride it is 397.2 eV (26), which is much lower than the E_b values of this line observed in this work. The mechanisms of NH_3 interaction with SiO_2 proposed in the literature can therefore not be applied to the present case.

A much lower temperature required for nitrogen bonding in mordenite may be explained by the high dispersion of the SiO_x species. The dimensions of the SiO_x clusters are limited by the dimensions of the main channel of mordenite (0.7×0.65 nm (27)) in which they are assumed to be localized. Moreover, we assume the presence of thermally nonstable OH groups on SiO_x which are easily removable at 400°C. To prove this hypothesis and elucidate the details of the coordination mode of N in thermally activated NH_4^+mordenite, further experiments are required.

5. CONCLUSIONS

Two lines can be distinguished in the N 1*s* photoelectron spectrum of ion-exchanged NH_4^+species in mordenite: the low-energy line at 400.0 eV belonging to NH_4^+ localized in the side pockets of mordenite, and the high-energy line at 403.2 eV, which belongs to NH_4^+ coordinated in its main channels. Most of the NH_4^+ cations are localized in the main channels of the mordenite (78%), the rest in the side pockets.

The H-mordenite prepared by heat activation of its NH_4^+ form at 400°C contains a substantial amount of atomic nitrogen. Its two forms can be distinguished by curve fitting of the N 1*s* photoelectron spectrum. Nitrogen atoms are most probably coordinated on oxygen vacancies of SiO_x clusters present in the channels of mordenite. The thermal desorption of ammonia from NH_4^+zeolites is thus a promising method of investigating their defect sites.

ACKNOWLEDGMENTS

We thank Dr. Zlatko Knor for a careful reading of the manuscript. This work was supported by the Grant Agency of the Czech Republic (Grants 104/00/1007 and 202/98/K002).

REFERENCES

1. Derouane, E. G., Lemos, F., Naccache, C., and Ribeiro, F. M. (Eds.), "Zeolite Microporous Solids: Synthesis, Structure, and Reactivity." Kluwer Academic, Dordrecht/Norwell, MA, 1991.
2. van Bekkum, H., Flanigen, E. M., and Jansen, J. C. (Eds.), "Introduction to Zeolite Science and Practice." Elsevier, Amsterdam, 1991.
3. Ernst, S., Hartmann, M., Sauerbeck, S., and Bongers, T., *Appl. Catal. A* **200**, 117 (2000).
4. Zecchina, A., Marchese, L., Bordiga, S, Paze, C., and Gianotti, E., *J. Phys. Chem. B* **101**, 10128 (1997).
5. Datka, J., Gil, B., and Kubacka, A., *Zeolites* **17**, 428 (1996).
6. Karge, H. G., *Z. Phys. Chem.* **76**, 133 (1971).
7. Zholobenko, V. I., Makarova, M. A., and Dwyer, J., *J. Phys. Chem.* **97**, 5962 (1993).

8. Ozin, G. A., Baker, M. D., Helwig, K., and Godber, J., *J. Phys. Chem.* **89**, 1846 (1985).
9. van Santen, R. A., and Kramer, G. J., *Chem. Rev.* **95**, 637 (1995).
10. Briggs, D., and Seah, M. P. (Eds.),"Practical Surface Analysis," 2nd ed., Vol. 1. Wiley, New York, 1990.
11. Kubelková, L., Kotrla, J., and Florian, J., *J. Phys. Chem.* **99**, 10285 (1995).
12. Remy, M. J., Genet, M. J., Notté, P. P., Lardinois, P. F., and Poncelet, G., *Microporous Mater.* **2**, 7 (1993).
13. Remy, M. J., Genet, M. J., Lardinois, P. F., Notté, P. P., and Poncelet, G., *Surf. Interface Anal.* **21**, 643 (1994).
14. Scofield, J., *J. Electron Spectrosc.* **8**, 129 (1976).
15. Kondo, N. J., Iizuka, M., and Domen, K., *Langmuir* **13**, 747 (1997).
16. Zecchina, A., Bordiga, S., Spoto, G., Scarano, D., Petrini, G., Leofanti, G., Padovan, M., and Otero Areán, C, *J. Chem. Soc. Faraday Trans.* **88**, 2959 (1992).
17. Ha, B. H., and Barthomeuf, D., *J. Chem. Soc., Faraday Trans. 1* **75**, 2366 (1979).
18. Jirka, I., *J. Phys. Chem. B* **105**, 1140 (2001).
19. Jirka, I., unpublished results.
20. Diebold, U., and Madey, T. E., *J. Vac. Sci. Technol. A* **10**, 2327 (1992).
21. Morrow, B. A., and Cody, I. A., *J. Phys. Chem.* **80**, 1998 (1976).
22. Morrow, B. A., Cody, I. A., and Lee, L. S., *J. Phys. Chem.* **79**, 2405 (1975).
23. Baumvol, I. J. R., Stedile, F. C., Ganem, J.-J., Trimaille, I., and Rigo, S., *J. Electrochem. Soc.* **143**, 1426 (1996).
24. Baumvol, I. J. R., Stedile, F. C., Ganem, J.-J., Trimaille, I., and Rigo, S., *J. Electrochem. Soc.* **143**, 2938 (1996).
25. Tanaka, K., Tsuge, A., Takiyama, M., and Shimizu, R., *Surf. Interface Anal.* **27**, 638 (1999).
26. Choo, C.-K., Sakamoto, T., Tanaka, K., and Nakata, R., *Appl. Surf. Sci.* **148**, 116 (1999).
27. Meier, W. M., Olson, D. H., and Baerlocher, Ch.,"Atlas of Zeolite Structure Types," 4th rev. ed. Elsevier, Amsterdam, 1996.
28. Wichterlová, B., Tvarůžková, Z., Sobalík, Z., and Sarv, P., *Microporous Mesoporous Mater.* **24**, 223 (1995).